



FEATURED ARTICLE

Predicting sporadic Alzheimer's disease progression via inherited Alzheimer's disease-informed machine-learning

Nicolai Franzmeier¹  | Nikolaos Koutsouleris² | Tammie Benzinger^{3,4} | Alison Goate^{5,6} | Celeste M. Karch^{4,7,8} | Anne M. Fagan^{4,7,9} | Eric McDade^{4,9} | Marco Duering¹ | Martin Dichgans^{1,10,11} | Johannes Levin^{10,11,12} | Brian A. Gordon^{4,13,14} | Yen Ying Lim¹⁵ | Colin L. Masters¹⁵ | Martin Rossor¹⁶ | Nick C. Fox¹⁶ | Antoinette O'Connor¹⁶ | Jasmeer Chhatwal¹⁷ | Stephen Salloway¹⁸ | Adrian Danek¹² | Jason Hassenstab^{4,9,14} | Peter R. Schofield^{19,20} | John C. Morris^{4,8,9} | Randall J. Bateman^{4,9} | the Alzheimer's disease neuroimaging initiative (ADNI)²¹ | the Dominantly Inherited Alzheimer Network (DIAN)²² | Michael Ewers¹ 

¹Institute for Stroke and Dementia Research, Klinikum der Universität München, Ludwig-Maximilians-Universität LMU, Munich, Germany

²Department of Psychiatry and Psychotherapy, Ludwig-Maximilians-Universität LMU, Munich, Germany

³Department of Radiology, Washington University in St. Louis, St. Louis, Missouri, USA

⁴Knight Alzheimer's Disease Research Center, Washington University in St. Louis, St. Louis, Missouri, USA

⁵Department of Genetics and Genomic Sciences, Icahn School of Medicine at Mount Sinai, New York, New York, USA

⁶Ronald M. Loeb Center for Alzheimer's Disease, Department of Neuroscience, Icahn School of Medicine at Mount Sinai, New York, New York, USA

⁷Hope Center for Neurological Disorders, Washington University in St. Louis, St. Louis, Missouri, USA

⁸Department of Psychiatry, Washington University in St. Louis, St. Louis, Missouri, USA

⁹Department of Neurology, Washington University in St. Louis, St. Louis, Missouri, USA

¹⁰Munich Cluster for Systems Neurology, Munich, Germany

¹¹German Center for Neurodegenerative Diseases (DZNE), Munich, Germany

¹²Department of Neurology, Ludwig-Maximilians-Universität München, Munich, Germany

¹³Mallinckrodt Institute of Radiology, Washington University, St. Louis, Missouri, USA

¹⁴Department of Psychological and Brain Sciences, Washington University, St. Louis, Missouri, USA

¹⁵The Florey Institute, The University of Melbourne, Parkville, Victoria, Australia

¹⁶Dementia Research Centre, University College London, Queen Square, London, UK

¹⁷Massachusetts General Hospital, Department of Neurology, Harvard Medical School, Boston, Massachusetts, USA

¹⁸Department of Neurology, Warren Alpert Medical School of Brown University, Providence, Rhode Island, USA

¹⁹Neuroscience Research Australia, Randwick, New South Wales, Australia

²⁰School of Medical Sciences, University of New South Wales, Sydney, New South Wales, Australia

²¹ADNI Consortium members are listed in the appendix

²²DIAN Consortium members are listed in the appendix

This is an open access article under the terms of the Creative Commons Attribution-NonCommercial License, which permits use, distribution and reproduction in any medium, provided the original work is properly cited and is not used for commercial purposes.

© 2020 The Authors. *Alzheimer's & Dementia* published by Wiley Periodicals, Inc. on behalf of Alzheimer's Association.

Correspondence

Michael Ewers, PhD, Institute for Stroke and Dementia Research (ISD), Klinikum der Universität München, Feodor-Lynen-Straße 17, Munich D-81377, Germany.
E-mail: michael.ewers@med.uni-muenchen.de

Abstract

Introduction: Developing cross-validated multi-biomarker models for the prediction of the rate of cognitive decline in Alzheimer's disease (AD) is a critical yet unmet clinical challenge.

Methods: We applied support vector regression to AD biomarkers derived from cerebrospinal fluid, structural magnetic resonance imaging (MRI), amyloid-PET and fluorodeoxyglucose positron-emission tomography (FDG-PET) to predict rates of cognitive decline. Prediction models were trained in autosomal-dominant Alzheimer's disease (ADAD, $n = 121$) and subsequently cross-validated in sporadic prodromal AD ($n = 216$). The sample size needed to detect treatment effects when using model-based risk enrichment was estimated.

Results: A model combining all biomarker modalities and established in ADAD predicted the 4-year rate of decline in global cognition ($R^2 = 24\%$) and memory ($R^2 = 25\%$) in sporadic AD. Model-based risk-enrichment reduced the sample size required for detecting simulated intervention effects by 50%–75%.

Discussion: Our independently validated machine-learning model predicted cognitive decline in sporadic prodromal AD and may substantially reduce sample size needed in clinical trials in AD.

KEYWORDS

Alzheimer's disease, autosomal-dominant Alzheimer's disease, biomarkers, machine learning, progression prediction, MRI, PET, risk enrichment

1 | BACKGROUND

Alzheimer's disease (AD) is characterized by amyloid-beta ($A\beta$) deposition, tau pathology, neurodegeneration, and cognitive decline.¹ Diagnosing and staging AD has been greatly facilitated by in vivo biomarkers including positron-emission tomography (PET) and cerebrospinal fluid (CSF) markers of $A\beta$ and pathologic tau, as well as volumetric magnetic resonance imaging (MRI) and fluorodeoxyglucose (FDG)-PET measures of neurodegeneration.² Apart from diagnosing AD, a clinically important challenge is predicting the worsening of cognitive impairment.³

Previous studies have shown that markers of primary AD pathology (ie, CSF $A\beta_{1-42}$, p-tau₁₈₁, $A\beta_{1-42}/p\text{-tau}_{181}$ ratio, amyloid-PET), neurodegeneration (structural MRI, FDG-PET), or biomarker combinations can predict future conversion from mild cognitive impairment (MCI) to AD dementia.^{4–9} The conversion from MCI to AD dementia is, however, a binary diagnostic categorization that does not capture the rate of cognitive change within the AD continuum.¹⁰ Biomarker-based point prediction of cognitive decline is, thus, a challenge to sufficiently power clinical trials via risk enrichment and to identify subjects at imminent risk of cognitive deterioration. Previous studies have shown that higher amyloid-PET,^{11,12} MRI-assessed hippocampal atrophy,¹³ FDG-PET hypometabolism,¹² and tau levels^{14,15} are associated with faster cognitive decline. Because biomarker combinations

can enhance the accuracy for predicting clinical progression,¹⁶ a critical yet unresolved question is how to merge multimodal and increasingly complex (eg, voxel-wise PET and MRI) data to maximize the prediction accuracy while keeping the number of assessments and costs low. Machine learning, which is instrumental for data mining,¹⁷ is well suited to identify biomarker sets for predicting cognitive decline. Here, recent machine-learning approaches to AD biomarker data showed that sets of imaging and CSF-derived markers discriminated MCI and AD patients from healthy controls¹⁸ and predicted the rate of future cognitive decline^{19,20} and time to symptom onset.²¹

A limitation of machine learning is, however, that algorithms may perform well in the sample they were trained on but rarely generalize to new data.^{22,23} To address this, previous studies have applied within-sample cross-validation (CV), in which a given sample is iteratively divided into training and test data to ensure that model training and testing are conducted on different datasets.^{18,24} While reducing the likelihood of overfitting, this approach leaves unaddressed the question whether the algorithm indeed generalizes to new and unseen data from independently recruited participants,²⁵ which is considered the gold standard of evaluating machine-learning performance.

Here, we aimed to establish a biomarker-based model to predict AD-related cognitive change rates, using validation across two independently recruited, deeply phenotyped AD samples. To this end, we first trained and cross-validated a support vector regression (SVR)

model using amyloid-PET, FDG-PET, structural MRI, and CSF data from 121 autosomal-dominant Alzheimer's disease (ADAD) subjects for predicting the estimated years to symptom onset (EYO), a proxy of cognitive decline. ADAD constitutes a unique training sample as the disease onset is at a relatively young age and the development of AD pathology and cognitive decline are not confounded by age-related comorbidities (eg, TDP-43, small-vessel disease).²⁶ Because in ADAD the time course of the development of dementia symptoms is strongly genetically driven, EYO can be used as a surrogate marker of AD-related cognitive decline.^{27–29} Here, we first trained biomarker-based machine-learning models for predicting EYO in ADAD. After model training and CV in ADAD, we tested whether the best model predicts up to 4-year cognitive decline when applied to an independent sample of 216 individuals with sporadic prodromal AD. Last, we tested whether machine learning-based selection of “at-risk” subjects can enhance the sensitivity to detect potential intervention effects and can reduce the required sample size in intervention studies.

2 | METHODS

2.1 | Participants

2.1.1 | Dominantly Inherited Alzheimer Network (DIAN)

We included 121 carriers of AD causative *PSEN1* and 2 or *APP* mutations (MC, data freeze 10), as well as 54 non-carrier siblings as healthy reference subjects for biomarker scaling (see supporting information). Subject inclusion required availability of baseline 3T T1-structural MRI, amyloid-PET (PiB), FDG-PET, and CSF data. No selection bias (ie, for age, sex, education) was found between the included and non-included subjects. EYO were defined as the difference between a participant's age at examination and the parental age of symptom onset. All participants provided written informed consent; local ethical approval was obtained at each participating DIAN site.

2.1.2 | Alzheimer's Disease Neuroimaging Initiative (ADNI)

Three hundred ninety-one individuals meeting Petersen criteria for amnesic MCI were included from ADNI, based on availability of baseline 3T T1-structural MRI, amyloid-PET (AV45), FDG-PET, CSF, and cognitive data (ie, ADNI-MEM and ADAS13), plus at least one (and up to four) annually consecutive cognitive follow-up assessments. No selection bias for age, sex, or education was found between the included and non-included ADNI subjects. $A\beta$ -status was determined using a pre-established global AV45-PET standard uptake value ratio (SUVR) cut-off of 1.11.³⁰ Cognitively normal $A\beta+$ subjects were not included, due to the few subjects meeting our inclusion criteria ($N = 50/46/8/0$ with 1/2/3/4-year follow-up). As a healthy reference group for biomarker scaling, we included baseline data of 49

RESEARCH IN CONTEXT

1. Systematic review: Prodromal Alzheimer's disease (AD) patients are at increased risk to develop AD dementia. However, there are considerable differences in cognitive decline rates between individuals, posing challenges for clinical prognostication. While AD biomarkers are established for diagnostics, there is an unmet need of biomarker models for predicting the rate of future cognitive decline.
2. Interpretation: Machine learning applied to complex AD biomarker data (ie, neuroimaging and biofluid) accurately predicted estimated symptom onset in autosomal-dominant Alzheimer's disease and generalized well to an independent sample of sporadic AD patients for predicting 1- to 4-year cognitive decline. Machine learning-based selection of at-risk patients with sporadic prodromal AD significantly reduced numbers required for detecting intervention effects by up to 50% to 75%. These findings suggest that machine learning may help derive meaningful prognostic indices from increasingly complex biomarker data.
3. Future direction: Does the addition of tau-positron emission tomography and neuroinflammatory biomarkers further increase prediction accuracy of future cognitive decline?

cognitively normal $A\beta$ -negative (ie, global AV45-PET SUVR < 1.11) subjects below the age of 70 scoring > 28 on the Mini-Mental State Exam (MMSE).

2.2 | Neuroimaging and biomarker assessment

Neuroimaging in DIAN and ADNI was performed using similar protocols initially developed for ADNI. Structural MRI has been recorded on 3T scanners with a spatial resolution of $1.1 \times 1.1 \times 1.2$ mm. FDG-PET has been acquired consistently in both samples (ie, 30 to 60 minutes after tracer injection, SUVR normalization to the brainstem), whereas Amyloid-PET scanning has been conducted using PiB in DIAN (40–70 minutes after tracer injection, SUVR normalized to the whole cerebellum) and AV45 in ADNI (50–70 minutes after tracer injection, SUVR normalized to the whole cerebellum). All ADNI^{31,32} and DIAN²⁹ imaging protocols have been described previously. For the current study, we used FreeSurfer-processed (Version 5.1) region of interest (ROI) data (ie, cortical thickness and subcortical volumes for structural MRI and SUVR values for PET) provided by the DIAN and ADNI neuroimaging cores. CSF concentrations of $A\beta_{1-42}$, phosphorylated tau at threonine 181 (p-tau₁₈₁), and total tau were measured by the using multiplex xMap Luminex in DIAN and via the Elecsys cobas e 601 instrument³³ in

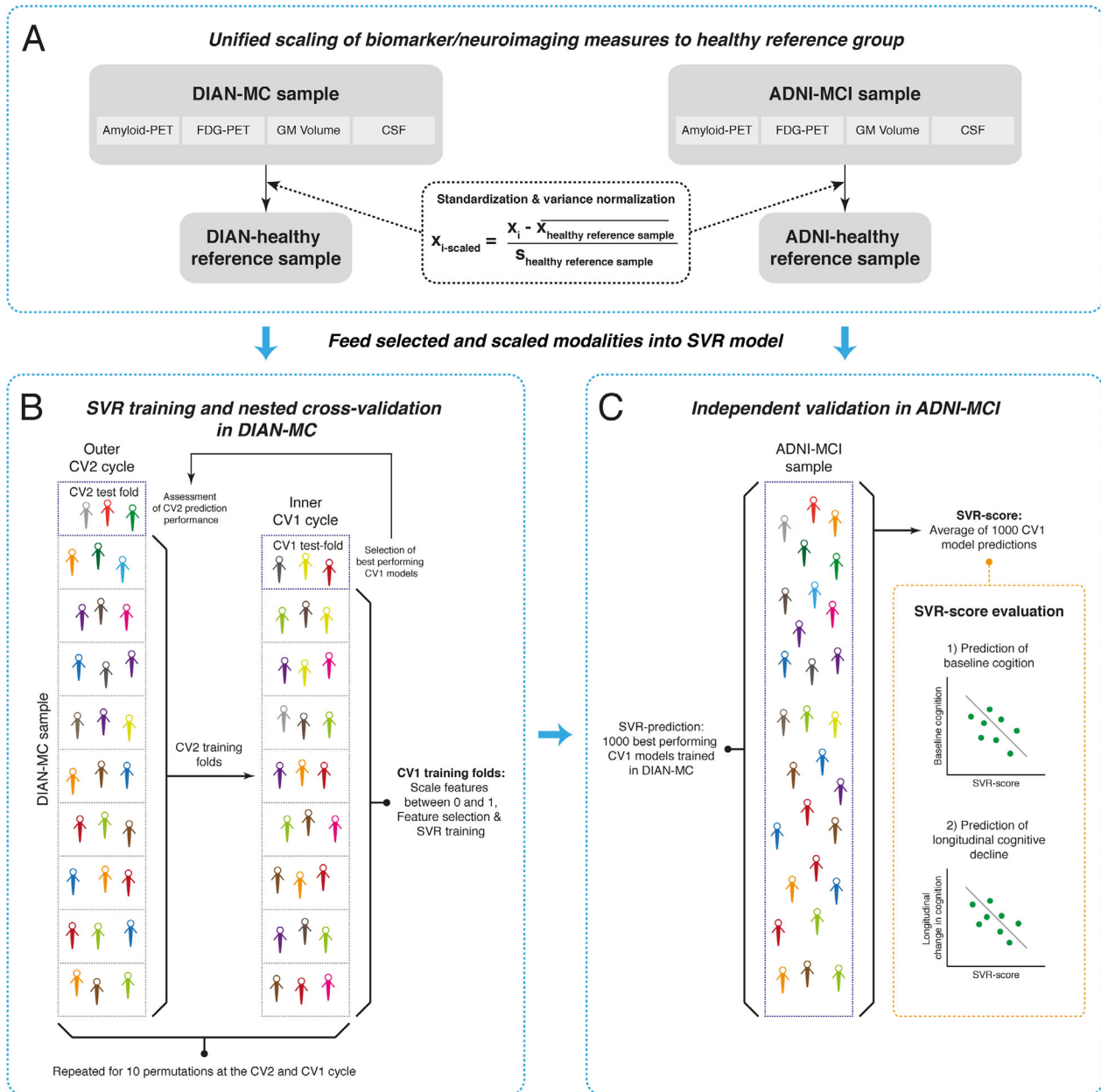


FIGURE 1 Flow-chart of the support vector regression (SVR) analysis pipeline. (A) Selected data from the DIAN-MC and ADNI-MCI sample are standardized and variance normalized to the respective healthy reference groups to ensure comparability of biomarker scaling across samples. (B) The SVR model is trained based on selected modalities in DIAN-MC in a nested cross-validation framework. (C) The trained SVR-models are blindly applied to the scaled ADNI-MCI biomarker data yielding a SVR score per subject. The SVR score is then evaluated as a predictor of baseline cognition and longitudinal cognitive decline in ADNI

ADNI. Details on biomarker assessments can be found in the supporting information.

2.3 | DIAN—support vector regression training and nested cross-validation

Machine-learning analysis was conducted using NeuroMiner, a Matlab-based machine-learning toolbox (www.pronia.eu/neurominer).^{34,35} In DIAN, we applied SVR to the neuroimaging/biomarker values

to predict EYO as a proxy of future cognitive decline. Prior to SVR analysis, all biomarker/neuroimaging values were scaled to a healthy reference sample within the ADNI and DIAN cohort, to yield comparably interpretable values across samples (see Figure 1A and supporting information). SVR training in DIAN (see Figure 1B) was conducted via repeated nested CV to obtain an unbiased SVR performance estimate in data unseen during SVR training. To this end, the DIAN MC group was randomly divided into 10 subsamples (ie, outer CV2-folds). During 10 iterations, a respective outer CV2 test fold was held out, while the remaining nine outer CV2-folds were pooled as SVR training data,

and randomly divided into 10 subsamples (inner CV1-folds). For 10 iterations, a respective inner CV1 test fold was held out, while the remaining inner CV1 data were used for SVR parameter tuning. The trained SVR parameters were then applied to the held-out inner CV1 test fold to estimate prediction performance in yet unseen data. For each CV1 iteration, the optimal SVR model was selected based on CV1 prediction performance (ie, minimum mean squared error between actual and SVR-predicted EYO). Last, the selected inner CV1 models were applied to the held-out outer CV2 test fold to estimate the mean CV2 prediction performance. This nested CV approach was complemented by repeated double CV, including 10-fold random permutation of the DIAN MC sample and repeating the above-described procedure for each permutation for CV1 and CV2 levels.³⁶ Together, feature selection and parameter optimization were performed on the CV1 level, while final SVR prediction performance was assessed exclusively on CV2 test folds unseen during SVR training (Figure 1B).

To extract the most predictive features (ie, imaging ROI values and CSF data), we performed feature selection at the CV1 level retaining the top 35% of features showing the highest Spearman correlation (ie, to minimize the influence of extreme values or skewed data) with EYO. Overall feature selection probability was defined as the likelihood of a given feature to be included across all optimal CV1 models. Altering the feature selection threshold between 25% and 45% did not change the overall result pattern reported below.

2.4 | Out-of-sample validation in ADNI

For our main analysis, we applied the 10000 ADAD-trained optimal CV1 SVR models to the ADNI MCI biomarker data, and computed the mean SVR score across all CV1 models, which we hypothesized to predict future cognitive decline (see Figure 1C).

2.5 | Statistics

Baseline measures were compared between groups using chi-squared tests for categorical variables and analysis of variance (ANOVAs; ADNI) or two-sample *t* tests (DIAN) for continuous measures.

In DIAN MC, we estimated SVR prediction performance for all possible modality combinations, by assessing Pearson-moment correlations between actual and SVR-predicted EYO. Feature selection probabilities were visualized for the SVR model including all modalities (ie, CSF [C], Amyloid-PET [A], FDG-PET [F], and GM [G]).

Next, we assessed whether SVR scores predicted baseline cognition or cognitive decline in the ADNI MCI validation sample. As measures of interest, we used ADNI-MEM, an established memory composite and ADAS13, a measure of global cognition.³⁷ Subject-specific cognitive change slopes were determined by fitting subject-specific linear models with ADNI-MEM or ADAS13 scores as the dependent variable and time from baseline as the independent variable. Annual cognitive changes were estimated for baseline to year 1, year 2, year 3, or year 4 for those subjects who had complete annual clinical follow-up data,

respectively. Using linear models controlled for age, sex, and education, we tested whether higher SVR scores predicted (1) stronger baseline cognitive impairment and (2) faster cognitive decline across 1- to 4-year follow-up. In an additional step, we included baseline cognition as a covariate to assess whether SVR scores predicted cognitive decline after accounting for baseline symptom severity. Analyses in ADNI MCI were stratified by $A\beta$ -status to test whether SVR-based prediction of cognition is specific for MCI- $A\beta+$ subjects.

Last, we tested whether SVR-based selection of MCI- $A\beta+$ subjects at risk of cognitive decline enhances the sensitivity to detect intervention effects. Using linear mixed models, we assessed the main effect of time from baseline on cognition (ie, ADNI-MEM or ADAS13) for the entire MCI- $A\beta+$ sample, or for SVR-selected subsamples of MCI- $A\beta+$ subjects at highest risk of cognitive decline (ie, showing above median SVR scores), controlling for age, sex, education, and random intercept. Following previous work,³⁸ sample size estimates were calculated on group-mean cognitive changes (ie, ADNI-MEM or ADAS13), with hypothetical 10%/20%/30%/40% intervention effects using the R-package *pwr* (settings: two-sample *t* test, two-tailed, type I error rate = 0.05, power = 0.8). Analyses were conducted for the best-performing SVR models with one, two, three, or four modality combinations for 1- to 4-year follow up.

All statistical analyses were performed in R statistical software. Effects were considered significant at a two-tailed alpha threshold of 0.05.

3 | RESULTS

Baseline characteristics of the study samples are presented in Table 1.

3.1 | SVR training and cross-validation in ADAD

The SVR model trained on all available modalities (ie, amyloid [A], FDG-PET [F], gray matter [G], CSF [C], abbreviated as AFGC) in DIAN MC accurately predicted EYO at the CV2 level ($r = 0.726$, $P < 0.0001$, $R^2 = 0.53$, Figure 2A). This model also showed the numerically highest predictive performance of EYO, compared to all other possible modality combinations (Table S1 in supporting information). For the AFGC model, we mapped the feature selection likelihood for each modality (Figure 2B). For amyloid-PET, almost the entire neocortex showed a high feature selection probability (ie, > 90%). For FDG-PET predominantly medial and lateral parietal and lateral frontal, ROIs showed high feature selection probability. For GM, mainly medial and lateral parietal and medial temporal, ROIs such as the hippocampus showed high feature selection probabilities. For CSF, p-tau₁₈₁ showed the highest selection probability, followed by total tau and $A\beta_{1-42}$. When restricting biomarker modalities for SVR training, the best-performing models for EYO prediction were AFG for three modalities ($r = 0.703$, $P < 0.0001$, $R^2 = 0.49$), AG for two modalities ($r = 0.677$, $P < 0.0001$, $R^2 = 0.46$), and G for single modality ($r = 0.628$, $P < 0.0001$, $R^2 = 0.39$).

TABLE 1 Baseline demographics

| DIAN | MC (N = 121) | NC (healthy reference) (N = 54) | P | |
|--------------------|----------------------|---------------------------------------|---------------------------------------|---------|
| Age | 38.66 (9.98) | 38.87 (10.48) | 0.8998 | |
| Sex (m/f) | 49/72 | 19/35 | 0.5056 | |
| Education | 14.27 (3.02) | 15.50 (2.23) | 0.0081 | |
| MMSE | 27.74 (7.88) | 30.00 (0.00) | 0.0365 | |
| Logical- memory | 11.44 (5.9) | 15.78 (3.45) | <0.0001 | |
| EYO | -7.10 (11.23) | -9.35 (10.94) | 0.2185 | |
| ADNI | MCI-Aβ+ (N = 216) | MCI-Aβ- (N = 175) | CN (healthy reference) (N = 49) | P |
| Age | 72.74 (6.69) | 70.16 (7.76) | 65.76 (2.69) | <0.0001 |
| Sex (m/f) | 117/99 | 94/81 | 23/26 | 0.6345 |
| Education | 16.00 (2.79) | 16.47 (2.47) | 17.14 (2.27) | 0.0139 |
| MMSE | 27.68 (1.83) | 28.54 (1.44) | 29.51 (0.51) | <0.0001 |
| ADAS13 | 17.18 (6.96) | 12.21 (5.48) | 6.24 (3.83) | <0.0001 |
| ADNI-MEM | 0.11 (0.63) | 0.62 (0.63) | 1.46 (0.61) | <0.0001 |

Values are displayed as mean (standard deviation). P-values for group comparisons are derived from two-sample t tests for DIAN and ANOVAs for ADNI for continuous measures and Chi-squared tests for categorical measures. Abbreviations: EYO, estimated years to symptom onset; MC, mutation carrier; MMSE, Mini-Mental State Exam; NC, non-carrier

3.2 | Independent validation in ADNI—Predicting cognitive decline in MCI-Aβ+

Next, we applied the ADAD-trained SVR model on all modalities (ie, AFGC) to ADNI MCI biomarker data. As hypothesized, greater AFGC scores predicted lower baseline ADNI-MEM ($t(211) = -6.692$, $\beta = -0.410$, $P < 0.0001$) and ADAS13 scores ($t(211) = 5.615$, $\beta = 0.355$, $P < 0.0001$) in the MCI-Aβ+ group but not in MCI-Aβ- (ADNI-MEM: $t(170) = -0.239$, $\beta = -0.017$, $P = 0.812$; ADAS13: $t(170) = 0.457$, $\beta = 0.035$, $P = 0.649$).

Most importantly, we found higher AFGC scores in MCI-Aβ+ to predict faster decline in ADNI-MEM consistently across all follow-up intervals, from baseline to year 1 ($t(211) = -4.547$, $\beta = -0.312$, $P < 0.0001$, Figure 3A), year 2 ($t(179) = -4.954$, $\beta = -0.361$, $P < 0.0001$, Figure 3B), year 3 ($t(140) = -5.240$, $\beta = -0.425$, $P < 0.0001$, Figure 3C), and year 4 ($t(100) = -5.317$, $\beta = -0.502$, $P < 0.0001$, Figure 3D) where partial R²-values increased for longer follow-up durations. Similarly, higher AFGC scores predicted decline in ADAS13 from baseline to year 1 ($t(211) = 2.337$, $\beta = 0.355$, $P = 0.0204$, Figure 3E), year 2 ($t(179) = 4.510$, $\beta = 0.334$, $P < 0.0001$, Figure 3F), year 3 ($t(140) = 4.756$, $\beta = 0.391$, $P < 0.0001$, Figure 3G), and year 4 ($t(100) = 5.143$, $\beta = 0.492$, $P < 0.0001$, Figure 3H). No association was found between SVR scores and cognitive changes in MCI-Aβ- suggesting specificity for Aβ+ subjects. All results are summarized in Table 2. Further, all above-listed results remained consistent when additionally controlling for baseline

cognition (ie, ADNI-MEM or ADAS13), suggesting that AFGC scores predict cognitive decline independent of baseline symptom severity (see Table S2 in supporting information).

3.3 | SVR-based selection of MCI-Aβ+ at risk of decline enhances the sensitivity to detect intervention effects

Next, we tested whether SVR-based selection of MCI-Aβ+ subjects at highest risk of cognitive decline (ie, defined as falling above the SVR score median) enhances the sensitivity to detect potential intervention effects. We first determined the main effect of time on longitudinal cognition (ADNI-MEM or ADAS13) in the unselected MCI-Aβ+ versus SVR-selected subsamples using linear mixed models, controlling for age, sex, education, and random intercept. Using the annual cognitive change scores, we estimated the required sample sizes to detect intervention effects of 10% to 40% at 1- to 4-year follow-up with an alpha of 0.05 at a power of 0.8. For the unselected MCI-Aβ+ sample, we found small but significant ADNI-MEM decreases across 1-year follow-up ($\beta = -0.052$, $P < 0.0001$, $R^2 = 0.01$). The sample size per arm to detect 10%/20%/30%/40% reduction in cognitive decline was 18984/4301/1737/892. In “at-risk” subjects with above median AFGC scores, we found a stronger effect of time on ADNI-MEM ($\beta = -0.109$, $P < 0.0001$, $R^2 = 0.053$). Here, the required N to detect 10%/20%/30%/40% reduction in cognitive decline was greatly reduced to 3375/765/310/159. Congruent results were found when performing these analyses for longer follow-up durations or for the best-performing three-modality, two-modality, and one-modality SVR models (AGC, AG, or G) for selection of at-risk subjects (see Table 3). Congruent results were also found when conducting all above-listed analyses using ADAS13 as measure of cognition (Table 3). Together, SVR-based “at-risk” selection may greatly reduce the required sample size to detect intervention effects.

4 | DISCUSSION

Our major aim was to establish a biomarker-based machine-learning model for point prediction of AD-related cognitive decline. Our first main finding was that machine-learning (ie, SVR) models trained for predicting future symptom manifestation in ADAD (ie, EYO) generalize well to sporadic AD, where we found high prediction accuracy for 1- to 4-year global cognitive and memory decline. Second, we show that SVR-based selection of sporadic AD subjects at highest risk for cognitive decline can drastically reduce patient numbers required for detecting intervention effects, even when using unimodal biomarkers. Together, our findings suggest that ADAD-informed and biomarker-based machine learning can accurately predict cognitive decline in sporadic AD and can be helpful for subject stratification in clinical trials.

Our findings make a significant contribution for identifying subjects at risk of imminent cognitive decline. Our results are validated across two independent and deeply phenotyped cohorts. A strength of the

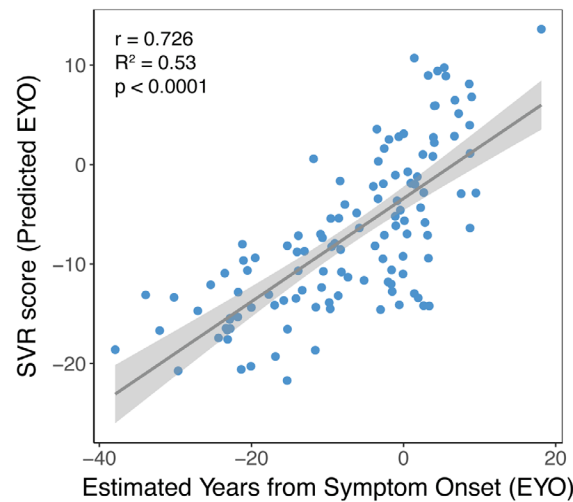
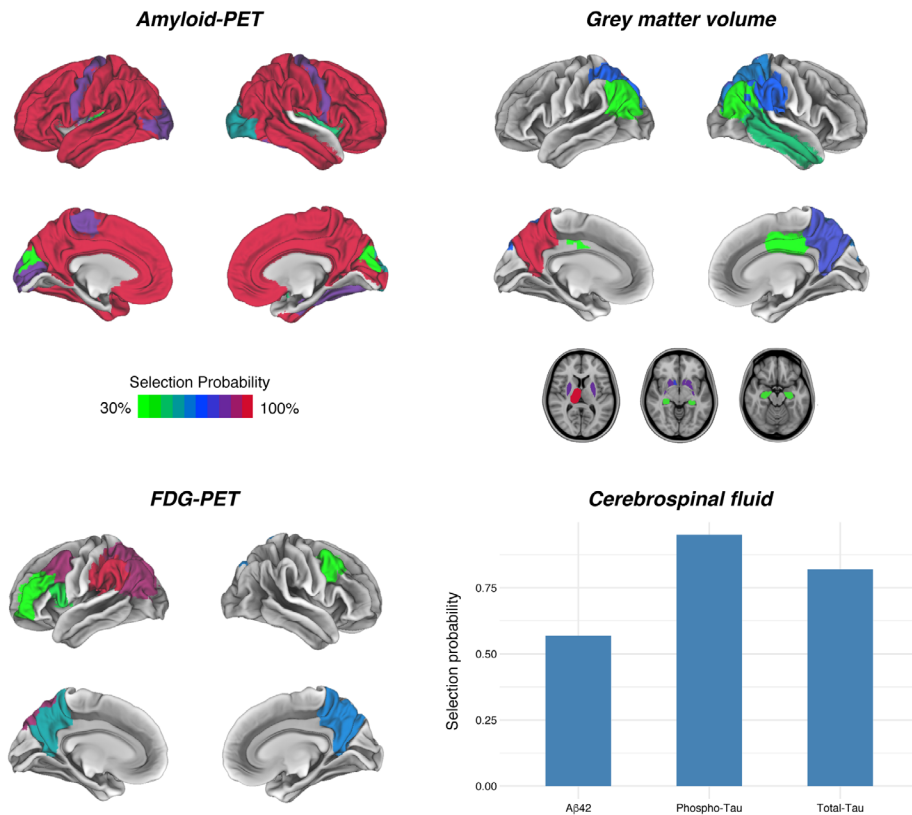
A: AFGC-based prediction of EYO in DIAN**B: Feature selection probabilities of the AFGC model**

FIGURE 2 SVR-based prediction of EYO in autosomal-dominant Alzheimer's disease and feature selection probabilities. (A) Scatterplot showing the association between observed EYO scores and AFGC-predicted estimated years to symptom onset (EYO) scores in DIAN-MC. (B) Selection probabilities of the AFGC model indicate the percentage of final CV1 models (see step in Figure 1B) that included the respective region of interest/biomarker. Features were selected in the DIAN-MC cohort during each CV1 cycle based on the correlation with the outcome measure (ie, EYO)

study is that we chose ADAD for model training, as those subjects are relatively young and age-related comorbidities (eg, small-vessel disease) are minimal.³⁹ This allowed extracting AD-specific brain changes that occur early in the disease course. We acknowledge differences between ADAD and sporadic AD including earlier symptom onset,

higher likelihood of non-memory symptoms,⁴⁰ and higher prevalence of psychiatric comorbidities⁴¹ in ADAD versus sporadic AD. However, both sporadic AD and ADAD share core neuropathological features and biomarker abnormalities including amyloid and tau accumulation, FDG-PET hypometabolism, and neurodegeneration.^{28,41} Importantly,

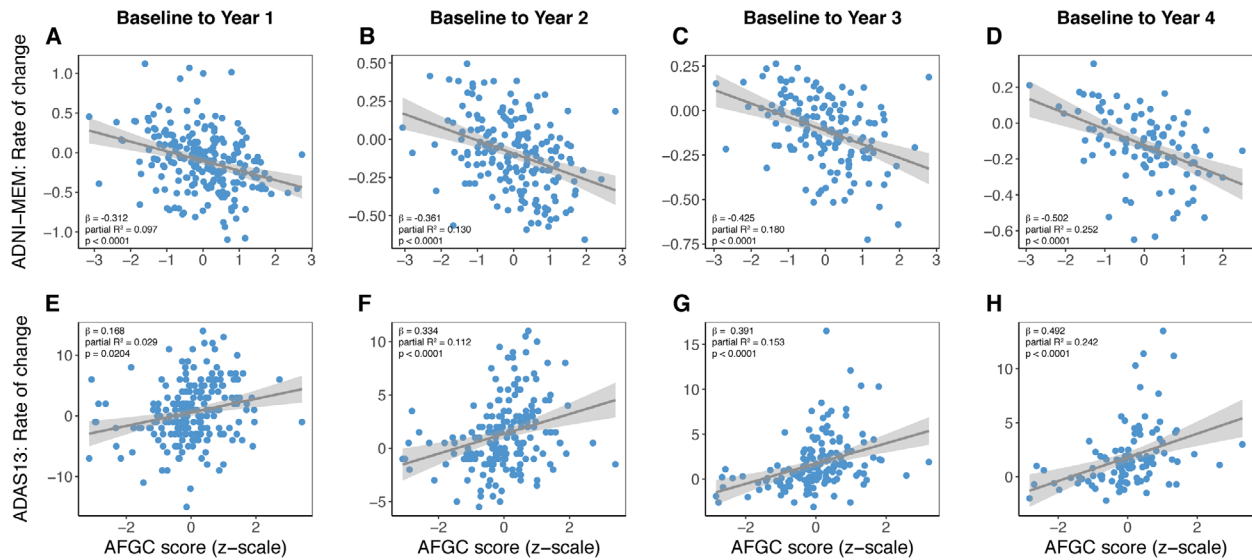


FIGURE 3 SVR-based prediction of cognitive changes in ADNI MCI-A β +. Scatterplots showing the association between AFGC-derived SVR scores and longitudinal cognitive change in ADNI-MCI-A β for ADNI-MEM (A-D) and ADAS13 (E-H). Standardized β -values, partial R^2 , and P -values are based on linear regression models adjusted for age, sex, and education

TABLE 2 Prediction of baseline cognition and longitudinal cognitive changes in ADNI MCI-A β +

| | ADNI MCI-A β + | | | | |
|----------|----------------------|---------|--------|---------|---------------|
| | N | β | T | P | Partial R^2 |
| ADNI-MEM | | | | | |
| Baseline | 216 | -0.410 | -6.692 | <0.0001 | 0.168 |
| Year 1 | 216 | -0.312 | -4.547 | <0.0001 | 0.097 |
| Year 2 | 184 | -0.361 | -4.954 | <0.0001 | 0.130 |
| Year 3 | 145 | -0.425 | -5.240 | <0.0001 | 0.180 |
| Year 4 | 105 | -0.502 | -5.317 | <0.0001 | 0.252 |
| ADAS-13 | | | | | |
| Baseline | 216 | 0.355 | 5.615 | <0.0001 | 0.126 |
| Year 1 | 216 | 0.168 | 2.337 | 0.0204 | 0.028 |
| Year 2 | 184 | 0.334 | 4.510 | <0.0001 | 0.112 |
| Year 3 | 145 | 0.391 | 4.746 | <0.0001 | 0.153 |
| Year 4 | 105 | 0.492 | 5.143 | <0.0001 | 0.242 |

All regression models were controlled for age, sex, and education.

the emergence of cognitive symptoms in ADAD is driven by AD pathology rather than age-related comorbidities, and thus, provides a good model for AD-related cognitive decline.^{27,42}

The most predictive features in amyloid-PET included almost the entire neocortex, sparing primary sensorimotor, and medial temporal regions that develop amyloid very late in AD.^{43,44} Further, predictive regions included posterior parietal and medial temporal regions for MRI and posterior parietal and lateral frontal regions for FDG-PET, that is, AD-typical predilection sites. Furthermore, the prediction of cognitive decline was non-significant in MCI-A β - and was independent of confounding factors including age, sex, education, or baseline cognition. Together, these findings support the validity of our prediction model to depend on key AD-related brain changes.

Previous studies evaluating biomarker combinations^{9,12} or machine learning demonstrated that biomarker combinations can enhance the accuracy of predicting cognitive decline or conversion to dementia.^{20,21} Consistently, we found increasing prediction accuracy as model estimation was informed by more biomarker modalities. We guarded against overfitting by first training and cross-validating the machine-learning algorithm on ADAD,⁴¹ with subsequent independent validation in sporadic AD. Importantly, in sporadic AD, we found that biomarker-based risk enrichment led to drastically lower sample sizes required to detect intervention effects with cognitive decline as an endpoint. This finding has several implications: First, screening examinations that are frequently used in intervention trials (eg, amyloid-PET and MRI) can be used to enrich for "at-risk" subjects to enhance power and reduce subject numbers and costs for interventions⁴⁵ or to assess whether intervention effects depend on individual progression risk.⁴⁶ Together, knowledge of individual risk for cognitive decline may be used for more adaptive and cost-efficient intervention research, which is urgently needed in view of numerous failed clinical trials in AD.⁴⁷

However, several caveats should be considered when interpreting our results: First, DIAN and ADNI differ in inclusion criteria (ADAD vs sporadic AD) and data acquisition protocols (ie, MRI hardware, PET tracers, and CSF immunoassays), reducing comparability across studies. To address this, we a priori adjusted all biomarker data to healthy control subjects within each study, to obtain harmonized and comparably interpretable values. Importantly, however, rather than pooling data across ADNI and DIAN, where variability across the two studies may hamper model estimation, we used an independent-validation approach for assessing external validity of the ADAD-trained SVR models. The high generalizability from ADAD to sporadic AD supports the robustness and external validity of the SVR models, suggesting that our findings are not driven by assessment procedures or study selection criteria.

TABLE 3 Sample size estimation for detecting intervention effects based on unselected MCI-A β + subject or on SVR selection of at-risk subjects (defined as falling above the median of SVR scores)

| Cognitive test | Group selection | Main effect of time on cognitive changes in MCI-A β + | | | | Required N per arm to detect an intervention effect of | | | | % Reduction of required N |
|------------------|-----------------|---|---------|---------|------------------------|--|-------|------|------|---------------------------|
| | | β | T | P | Partial R ² | 10% | 20% | 30% | 40% | |
| 1-year follow-up | | | | | | | | | | |
| ADNI-MEM | No selection | -0.052 | -4.021 | <0.0001 | 0.010 | 18984 | 4301 | 1737 | 892 | NA |
| | G-risk | -0.084 | -4.703 | <0.0001 | 0.028 | 6937 | 1572 | 635 | 327 | 63% |
| | AG-risk | -0.090 | -5.170 | <0.0001 | 0.033 | 5742 | 1301 | 526 | 271 | 70% |
| | AGC-risk | -0.095 | -5.574 | <0.0001 | 0.037 | 4940 | 1120 | 458 | 233 | 74% |
| | AFGC-risk | -0.109 | -6.744 | <0.0001 | 0.053 | 3375 | 765 | 310 | 159 | 82% |
| ADAS13 | No selection | 0.037 | 1.764 | 0.0792 | 0.002 | 94800 | 21475 | 8672 | 4453 | NA |
| | G-risk | 0.070 | 2.317 | 0.0224 | 0.008 | 27638 | 6261 | 2529 | 1299 | 71% |
| | AG-risk | 0.073 | 2.326 | 0.0219 | 0.009 | 27392 | 6205 | 2506 | 1287 | 71% |
| | AGC-risk | 0.089 | 2.933 | 0.0041 | 0.013 | 17335 | 3927 | 1586 | 815 | 82% |
| | AFGC-risk | 0.100 | 3.149 | 0.0021 | 0.016 | 15086 | 3418 | 1381 | 709 | 84% |
| 2-year follow-up | | | | | | | | | | |
| ADNI-MEM | No selection | -0.076 | -6.425 | <0.0001 | 0.026 | 9166 | 2077 | 839 | 431 | NA |
| | G-risk | -0.131 | -8.071 | <0.0001 | 0.080 | 2741 | 622 | 252 | 130 | 70% |
| | AG-risk | -0.136 | -8.372 | <0.0001 | 0.085 | 2574 | 584 | 236 | 122 | 72% |
| | AGC-risk | -0.140 | -8.862 | <0.0001 | 0.095 | 2370 | 538 | 218 | 112 | 74% |
| | AFGC-risk | -0.144 | -8.850 | <0.0001 | 0.097 | 2293 | 520 | 211 | 109 | 75% |
| ADAS13 | No selection | 0.122 | 6.421 | <0.0001 | 0.031 | 8748 | 1982 | 801 | 412 | NA |
| | G-risk | 0.178 | 6.208 | <0.0001 | 0.060 | 4360 | 988 | 400 | 206 | 50% |
| | AG-risk | 0.178 | 6.137 | <0.0001 | 0.060 | 4545 | 1030 | 417 | 214 | 48% |
| | AGC-risk | 0.199 | 6.957 | <0.0001 | 0.075 | 3526 | 799 | 323 | 166 | 60% |
| | AFGC-risk | 0.209 | 7.160 | <0.0001 | 0.081 | 3410 | 773 | 313 | 161 | 61% |
| 4-year follow-up | | | | | | | | | | |
| ADNI-MEM | No selection | -0.173 | -10.755 | <0.0001 | 0.107 | 3857 | 874 | 354 | 182 | NA |
| | G-risk | -0.264 | -12.331 | <0.0001 | 0.250 | 1348 | 306 | 124 | 64 | 65% |
| | AG-risk | -0.291 | -14.188 | <0.0001 | 0.307 | 905 | 206 | 84 | 43 | 76% |
| | AGC-risk | -0.294 | -14.303 | <0.0001 | 0.318 | 900 | 205 | 83 | 43 | 76% |
| | AFGC-risk | -0.264 | -12.694 | <0.0001 | 0.256 | 1295 | 294 | 119 | 62 | 66% |
| ADAS13 | No selection | 0.239 | 10.750 | <0.0001 | 0.118 | 3818 | 866 | 350 | 180 | NA |
| | G-risk | 0.325 | 10.943 | <0.0001 | 0.222 | 1778 | 404 | 163 | 84 | 53% |
| | AG-risk | 0.356 | 11.921 | <0.0001 | 0.348 | 1462 | 332 | 135 | 69 | 62% |
| | AGC-risk | 0.369 | 11.919 | <0.0001 | 0.262 | 1441 | 327 | 133 | 68 | 62% |
| | AFGC-risk | 0.338 | 11.302 | <0.0001 | 0.235 | 1728 | 392 | 159 | 82 | 54% |

Second, the sporadic AD group was restricted to MCI; hence, it remains open whether our findings generalize toward earlier AD stages. However, previous studies have shown that preclinical AD subjects show only little cognitive change across 1- to 4-year follow-up intervals;⁴⁸ hence, we reason that longer follow-ups and large numbers currently unavailable in ADNI are required to test whether the SVR model can predict cognitive changes in preclinical AD.

Third, we trained the model on EYO in ADAD, which is only a cross-sectional proxy of future cognitive decline.²⁷ Computing actual cognitive decline in ADAD would have drastically reduced the sample

size to those with available longitudinal cognitive data. To maximize sample size, which is critical for training and CV of machine-learning models within the ADAD group, we thus preferred to use cross-sectional data.⁴⁹ When sufficient longitudinal data become available in DIAN, future studies may assess whether SVR performance can be further improved when the SVR model is trained on actual longitudinal cognitive decline.

Fourth, due to limited data availability, we did not include tau-PET, which has been recently shown to be a good predictor of future cognitive decline in AD.¹⁵ However, we included measures of

tau-related pathology (ie, CSF), which have been previously shown to correlate with the level of tau-PET uptake⁵⁰ and to predict future cognitive decline.⁹ Nevertheless, inclusion of tau-PET in the SVR model may improve prediction of cognitive decline. Here, our methodological framework will easily allow us to include tau-PET as an additional modality as soon as large enough data become available.

Together, we show that ADAD-informed machine learning can be powerful for point prediction of future cognitive decline in sporadic AD. These findings have important implications because our proposed SVR models may help derive single prognostic indices from increasingly complex biomarker data. The proposed models allow flexible inclusion of various biomarkers, rendering them highly adaptable to individual cohorts. To enhance the external validity of our proposed SVR models, it will be of special importance in the future to determine their prediction performance also across less selective and community-based samples, as well as across different biomarker combinations and acquisition protocols. Our findings may be critical for clinical AD research to identify subjects at risk for progression and to evaluate therapeutic interventions for future cognitive decline.

ACKNOWLEDGMENTS

Data collection and sharing for this project was supported by the Dominantly Inherited Alzheimer's Network (DIAN, UF1AG032438) funded by the National Institute on Aging (NIA), the German Center for Neurodegenerative Diseases (DZNE), Raul Carrea Institute for Neurological Research (FLENI), partial support by the Research and Development Grants for Dementia from Japan Agency for Medical Research and Development, AMED, and the Korea Health Technology R&D Project through the Korea Health Industry Development Institute (KHIDI). This manuscript has been reviewed by DIAN Study investigators for scientific content and consistency of data interpretation with previous DIAN Study publications. We acknowledge the altruism of the participants and their families and contributions of the DIAN research and support staff at each of the participating sites for their contributions to this study. The study was funded by grants from the Alzheimer Forschung Initiative (AFI, Grant 15035 to Michael Ewers) and European Commission (Grant 334259 to Michael Ewers). ADNI data collection and sharing for this project was funded by the ADNI (National Institutes of Health Grant U01 AG024904) and DOD ADNI (Department of Defense award number W81XWH-12-2-0012). ADNI is funded by the National Institute on Aging, the National Institute of Biomedical Imaging, and Bioengineering, and through contributions from the following: AbbVie; Alzheimer's Association; Alzheimer's Drug Discovery Foundation; Araclon Biotech; BioClinica, Inc.; Biogen; Bristol-Myers Squibb Company; CereSpir, Inc.; Cogstate; Eisai, Inc.; Elan Pharmaceuticals, Inc.; Eli Lilly and Company; EuroImmun; F. Hoffmann-La Roche Ltd and its affiliated company Genentech, Inc.; Fujirebio; GE Healthcare; IXICO Ltd.; Janssen Alzheimer Immunotherapy Research & Development, LLC; Johnson & Johnson Pharmaceutical Research & Development LLC; Lumosity; Lundbeck; Merck & Co., Inc.; Meso Scale Diagnostics, LLC; NeuroRx Research; Neurotrack Technologies; Novartis Pharmaceuticals Corporation; Pfizer Inc.; Piramal Imaging; Servier; Takeda Pharmaceutical Company; and Transition

Therapeutics. The Canadian Institutes of Health Research is providing funds to support ADNI clinical sites in Canada. Private-sector contributions are facilitated by the Foundation for the National Institutes of Health (www.fnih.org).

NCF acknowledges support from the MRC, the NIHR UCLH Biomedical Research Centre, and the UK Dementia Research Institute at UCL.

AUTHOR CONTRIBUTIONS

NF preprocessed the imaging data, designed the study, performed statistical analysis and interpreted the results, and wrote the manuscript; NK supervised the data analysis and critically revised the manuscript; TB, AG, CMK, AMF, EM, MD, MD, JL, BAG, YYL, CLM, MR, NCF, AOC, JC, SS, AD, JH, PRS, JCM, and RJB contributed data and critically revised the manuscript; ME designed the study, interpreted the results, and wrote the manuscript.

ORCID

Nicolai Franzmeier  <https://orcid.org/0000-0001-9736-2283>

Michael Ewers  <https://orcid.org/0000-0001-5231-1714>

REFERENCES

- Selkoe DJ, Hardy J. The amyloid hypothesis of Alzheimer's disease at 25 years. *EMBO Mol Med*. 2016;8:595-608.
- Jack CR, Jr., Bennett DA, Blennow K, et al. NIA-AA research framework: toward a biological definition of Alzheimer's disease. *Alzheimers Dement*. 2018;14:535-562.
- Barnes DE, Lee SJ. Predicting Alzheimer's risk: why and how? *Alzheimers Res Ther*. 2011;3:33.
- Dickerson BC, Wolk DA, Alzheimer's Disease Neuroimaging Initiative. Biomarker-based prediction of progression in MCI: comparison of AD signature and hippocampal volume with spinal fluid amyloid-beta and tau. *Front Aging Neurosci*. 2013;5:55.
- Jack CR, Jr., Wiste HJ, Vemuri P, et al. Brain beta-amyloid measures and magnetic resonance imaging atrophy both predict time-to-progression from mild cognitive impairment to Alzheimer's disease. *Brain*. 2010;133:3336-3348.
- Hinrichs C, Singh V, Xu G, Johnson SC, Alzheimer's Disease Neuroimaging Initiative. Predictive markers for AD in a multi-modality framework: an analysis of MCI progression in the ADNI population. *Neuroimage*. 2011;55:574-589.
- Mattsson N, Zetterberg H, Hansson O, et al. CSF biomarkers and incipient Alzheimer disease in patients with mild cognitive impairment. *JAMA*. 2009;302:385-393.
- Ewers M, Buerger K, Teipel SJ, et al. Multicenter assessment of CSF-phosphorylated tau for the prediction of conversion of MCI. *Neurology*. 2007;69:2205-2212.
- Frolich L, Peters O, Lewczuk P, et al. Incremental value of biomarker combinations to predict progression of mild cognitive impairment to Alzheimer's dementia. *Alzheimers Res Ther*. 2017;9:84.
- Aisen PS, Cummings J, Jack CR, Jr., et al. On the path to 2025: understanding the Alzheimer's disease continuum. *Alzheimers Res Ther*. 2017;9:60.
- Farrell ME, Kennedy KM, Rodrigue KM, et al. Association of longitudinal cognitive decline with amyloid burden in middle-aged and older adults: evidence for a dose-response relationship. *JAMA Neurol*. 2017;74:830-838.
- Landau SM, Mintun MA, Joshi AD, et al. Amyloid deposition, hypometabolism, and longitudinal cognitive decline. *Ann Neurol*. 2012;72:578-586.

13. Velayudhan L, Proitsi P, Westman E, et al. Entorhinal cortex thickness predicts cognitive decline in Alzheimer's disease. *J Alzheimers Dis*. 2013;33:755-766.
14. Soldan A, Pettigrew C, Cai Q, et al. Hypothetical preclinical Alzheimer disease groups and longitudinal cognitive change. *JAMA Neurol*. 2016;73:698-705.
15. Aschenbrenner AJ, Gordon BA, Benzinger TLS, Morris JC, Hassenstab JJ. Influence of tau PET, amyloid PET, and hippocampal volume on cognition in Alzheimer disease. *Neurology*. 2018;91:e859-e866.
16. Wolk DA, Sadowsky C, Safirstein B, et al. Use of flutemetamol F 18-labeled positron emission tomography and other biomarkers to assess risk of clinical progression in patients with amnesic mild cognitive impairment. *JAMA Neurol*. 2018;75:1114-1123.
17. Lemm S, Blankertz B, Dickhaus T, Muller KR. Introduction to machine learning for brain imaging. *Neuroimage*. 2011;56:387-399.
18. Casanova R, Hsu FC, Sink KM, et al. Alzheimer's disease risk assessment using large-scale machine learning methods. *PLoS One*. 2013;8:e77949.
19. Choi H, Jin KH, Alzheimer's Disease Neuroimaging Initiative. Predicting cognitive decline with deep learning of brain metabolism and amyloid imaging. *Behav Brain Res*. 2018;344:103-109.
20. Bhagwat N, Viviano JD, Voineskos AN, Chakravarty MM, Alzheimer's Disease Neuroimaging Initiative. Modeling and prediction of clinical symptom trajectories in Alzheimer's disease using longitudinal data. *PLoS Comput Biol*. 2018;14:e1006376.
21. Vogel JW, Vachon-Preseau E, Pichet Binette A, et al. Brain properties predict proximity to symptom onset in sporadic Alzheimer's disease. *Brain*. 2018;141:1871-1883.
22. Handelman GS, Kok HK, Chandra RV, et al. Peering into the black box of artificial intelligence: evaluation metrics of machine learning methods. *AJR Am J Roentgenol*. 2019;212:38-43.
23. Wong T-T. Performance evaluation of classification algorithms by k-fold and leave-one-out cross validation. *Pattern Recognit*. 2015;48:2839-2846.
24. Ritter K, Schumacher J, Weygandt M, Buchert R, Allefeld C, Haynes JD. Multimodal prediction of conversion to Alzheimer's disease based on incomplete biomarkers. *Alzheimers Dement (Amst)*. 2015;1:206-215.
25. Plant C, Teipel SJ, Oswald A, et al. Automated detection of brain atrophy patterns based on MRI for the prediction of Alzheimer's disease. *Neuroimage*. 2010;50:162-174.
26. Ryman DC, Acosta-Baena N, Aisen PS, et al. Symptom onset in autosomal dominant Alzheimer disease: a systematic review and meta-analysis. *Neurology*. 2014;83:253-260.
27. McDade E, Wang G, Gordon BA, et al. Longitudinal cognitive and biomarker changes in dominantly inherited Alzheimer disease. *Neurology*. 2018;91:e1295-e1306.
28. Bateman RJ, Aisen PS, De Strooper B, et al. Autosomal-dominant Alzheimer's disease: a review and proposal for the prevention of Alzheimer's disease. *Alzheimers Res Ther*. 2011;3:1.
29. Benzinger TL, Blazey T, Jack CR, Jr., et al. Regional variability of imaging biomarkers in autosomal dominant Alzheimer's disease. *Proc Natl Acad Sci U S A*. 2013;110:E4502-E4509.
30. Landau SM, Breault C, Joshi AD, et al. Amyloid-beta imaging with Pittsburgh compound B and florbetapir: comparing radiotracers and quantification methods. *J Nucl Med*. 2013;54:70-77.
31. Jack CR, Jr., Barnes J, Bernstein MA, et al. Magnetic resonance imaging in Alzheimer's Disease Neuroimaging Initiative 2. *Alzheimers Dement*. 2015;11:740-756.
32. Jagust WJ, Landau SM, Koeppe RA, et al. The Alzheimer's Disease Neuroimaging Initiative 2 PET Core: 2015. *Alzheimers Dement*. 2015;11:757-771.
33. Bittner T, Zetterberg H, Teunissen CE, et al. Technical performance of a novel, fully automated electrochemiluminescence immunoassay for the quantitation of beta-amyloid (1-42) in human cerebrospinal fluid. *Alzheimers Dement*. 2016;12:517-526.
34. Koutsouleris N, Kambeitz-Illankovic L, Ruhrmann S, et al. Prediction models of functional outcomes for individuals in the clinical high-risk state for psychosis or with recent-onset depression: a multimodal, multisite machine learning analysis. *JAMA Psychiatry*. 2018;75:1156-1172.
35. Dwyer DB, Falkai P, Koutsouleris N. Machine learning approaches for clinical psychology and psychiatry. *Annu Rev Clin Psychol*. 2018;14:91-118.
36. Filzmoser P, Liebmann B, Varmuza K. Repeated double cross validation. *J Chemom*. 2009;23:160-171.
37. Crane PK, Carle A, Gibbons LE, et al. Development and assessment of a composite score for memory in the Alzheimer's Disease Neuroimaging Initiative (ADNI). *Brain Imaging Behav*. 2012;6:502-516.
38. Baykara E, Gesierich B, Adam R, et al. A novel imaging marker for small vessel disease based on skeletonization of white matter tracts and diffusion histograms. *Ann Neurol*. 2016;80:581-592.
39. Ringman JM, Monsell S, Ng DW, et al. Neuropathology of autosomal dominant Alzheimer disease in the National Alzheimer Coordinating Center database. *J Neuropathol Exp Neurol*. 2016;75:284-290.
40. Joshi A, Ringman JM, Lee AS, Juarez KO, Mendez MF. Comparison of clinical characteristics between familial and non-familial early onset Alzheimer's disease. *J Neurol*. 2012;259:2182-2188.
41. Day GS, Musiek ES, Roe CM, et al. Phenotypic similarities between late-onset autosomal dominant and sporadic Alzheimer disease: a single-family case-control study. *JAMA Neurol*. 2016;73:1125-1132.
42. Bateman RJ, Xiong C, Benzinger TL, et al. Clinical and biomarker changes in dominantly inherited Alzheimer's disease. *N Engl J Med*. 2012;367:795-804.
43. Grothe MJ, Barthel H, Sepulcre J, et al. In vivo staging of regional amyloid deposition. *Neurology*. 2017;89:2031-2038.
44. Quiroz YT, Sperling RA, Norton DJ, et al. Association between amyloid and tau accumulation in young adults with autosomal dominant Alzheimer disease. *JAMA Neurol*. 2018;75:548-556.
45. Ansart M, Epelbaum S, Gagliardi G, et al. Reduction of recruitment costs in preclinical AD trials: validation of automatic pre-screening algorithm for brain amyloidosis. *Stat Methods Med Res*. 2019;962280218823036.
46. Gold M. Phase II clinical trials of anti-amyloid beta antibodies: when is enough, enough? *Alzheimers Dement (N Y)*. 2017;3:402-409.
47. Cummings J, Lee G, Ritter A, Zhong K. Alzheimer's disease drug development pipeline: 2018. *Alzheimers Dement (N Y)*. 2018;4:195-214.
48. Roberts RO, Aakre JA, Kremers WK, et al. Prevalence and outcomes of amyloid positivity among persons without dementia in a longitudinal, population-based setting. *JAMA Neurol*. 2018;75:970-979.
49. Mateos-Perez JM, Dadar M, Lacalle-Aurioles M, Iturria-Medina Y, Zeighami Y, Evans AC. Structural neuroimaging as clinical predictor: a review of machine learning applications. *Neuroimage Clin*. 2018;20:506-522.
50. La Joie R, Bejanin A, Fagan AM, et al. Associations between [(18)F]AV1451 tau PET and CSF measures of tau pathology in a clinical sample. *Neurology*. 2018;90:e282-e290.

SUPPORTING INFORMATION

Additional supporting information may be found online in the Supporting Information section at the end of the article.

How to cite this article: Franzmeier N, Koutsouleris N, Benzinger T, et al. Predicting sporadic Alzheimer's disease progression via inherited Alzheimer's disease-informed machine-learning. *Alzheimer's Dement*. 2020;16:501-511. <https://doi.org/10.1002/alz.12032>